Rosas-Laverde, NM.; Pruna, AI.; Busquets Mataix, DJ.; Marí, B.; Cembrero Cil, J.; Salas Vicente, F.; Orozco-Messana, J. (2018). Improving the properties of Cu2O/ZnO heterojunction for photovoltaic application by graphene oxide. Ceramics International. 44(18):23045-23051. https://doi.org/10.1016/j.ceramint.2018.09.107

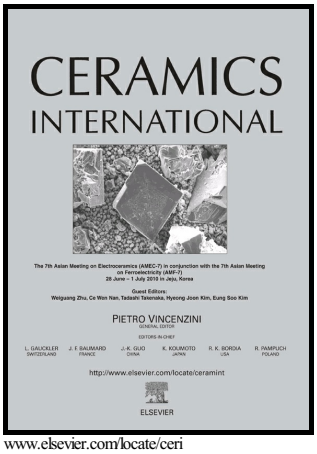

www.elsevier.com/locate/ceri

Improving the properties of Cu_2O/ZnO heterojunction for photovoltaic application by graphene oxide

N.M. Rosas-Laverde, A. Pruna, D. Busquets-Mataix, B. Marí, J. Cembrero, F. Salas Vicente, J. Orozco-Messana

PII: S0272-8842(18)32572-0
DOI: https://doi.org/10.1016/j.ceramint.2018.09.107
Reference: CERI19506

To appear in: *Ceramics International*

Received date: 5 June 2018
Revised date: 4 August 2018
Accepted date: 11 September 2018

Cite this article as: N.M. Rosas-Laverde, A. Pruna, D. Busquets-Mataix, B. Marí, J. Cembrero, F. Salas Vicente and J. Orozco-Messana, Improving the properties of Cu_2O/ZnO heterojunction for photovoltaic application by graphene oxide, *Ceramics International,* https://doi.org/10.1016/j.ceramint.2018.09.107

Improving the properties of Cu_2O/ZnO heterojunction for photovoltaic application by graphene oxide

N.M. Rosas-Laverde[1,2], A. Pruna[3,4*], D. Busquets-Mataix[1], B. Marí[5], J. Cembrero[1], F. Salas Vicente[1], J. Orozco-Messana[1]

[1]Department of Materials and Mechanical Engineering, Universitat Politècnica de València, Valencia, Spain

[2]Department of Materials, Escuela Politécnica Nacional, Quito, Ecuador

[3]Center for Surface Science and Nanotechnology, Polytechnic University of Bucharest, Bucharest, Romania

[4]Instituto de Tecnología de Materiales, Universitat Politècnica de València, Valencia, Spain

[5]Department of Applied Physics, Universitat Politècnica de València, Valencia, Spain

[*]Corresponding autor: ai.pruna@gmail.com

Abstract:

A p-Cu_2O/n-ZnO heterojunction grown on fluorine-doped tin oxide (FTO) substrate is reported by a combined low-cost approach employing tape-casting of ZnO layer and subsequent electrochemical deposition of Cu_2O layer. Graphene oxide (GO) nanosheets were employed as nanofiller for the ZnO matrix. Moreover, a ZnO buffer layer was inserted at the interface between the Cu_2O and ZnO layers. The morphological, structural and photoelectrical characteristics of these heterojunction layers were investigated by field emission scanning electron microscopy (FESEM), X-ray diffraction (XRD), Raman spectroscopy and photoelectrical current-voltage measurements. The results confirmed that the morphology and structure of ZnO layer were affected by the incorporation of GO nanosheets while the presence of buffer layer influenced the growth of Cu_2O layer. This work shows the addition of GO and the use of ZnO buffer layer represent a viable approach towards improving the photoelectrical properties of the Cu_2O/ZnO heterojunction cell.

Keywords:

Tape-casting; Electrodeposition; Heterojunction; ZnO; Cu_2O; Graphene oxide

1. Introduction

Given the worsening of the environmental conditions, the generation of electricity from non-polluting, renewable and inexpensive sources has attracted much interest. Solar energy is considered to be the cleanest and least limiting source of energy. It can be converted into electricity by the use of photovoltaic devices, such as solar cells. Amongst the solar cells employed in the present, the heterojunction ones such as those based on Cu_2O or ZnO layers have attracted significant interest due to the ease in fabrication of electrodes and the amount of light energy produced with relatively low voltage generated [1].

Zinc oxide (ZnO) is an n-type semiconductor with a band gap of 3.37 eV that can be employed as a window layer in the solar cell, due to its excellent optical and electrical properties. Several synthesis methods including magnetron sputtering, chemical vapor deposition, pulsed laser deposition, electrochemical deposition etc. have been employed for the fabrication of ZnO electrode [2–4]. Amongst these methods, doctor Blade or tape-casting method is a fast, easy and economically viable method to produce thin films at large scale [5–7]. This method consists in the preparation of a dense paste containing a suspension of ceramic powders in organic solvents, plasticizers and binders. Films of controlled thickness and width are further obtained by blade-spreading the paste on a surface. Upon the solvent evaporation and sintering treatment, a solid film is obtained [8, 9]. This method is useful to synthesize ceramic layers for a wide range of applications including capacitors, combustion cells or dye sensitized solar cells [7, 10–13].

Designing ZnO porous films is an important challenge in order to improve the light collection. Namely, by adding the reduced graphene oxide (rGO) to the ZnO active layer, the ZnO bandgap decreases thus resulting in improved performance of the solar cell [14]. Graphene oxide (GO) - a fascinating two-dimensional carbon nanomaterial decorated with oxygen functional groups can be exploited for fabricating composites thanks to its hydrophilicity [15]. However, the presence of such groups is known to result in a low conductivity, thus, they must be removed via different reduction processes including chemical or electrochemical reduction [16].

On the other hand, the cuprous oxide (Cu_2O) is a non-toxic, abundant, inexpensive and intrinsically p-type semiconductor with a high absorption coefficient, a band gap of about 2.1 eV and an estimated theoretical conversion solar efficiency of 12%.

Techniques including electrodeposition, thermal oxidation of copper metal, spraying, pulsed laser deposition, or chemical vapor deposition [1, 3, 17–19] are currently applied for the synthesis of Cu_2O. Amongst these techniques, electrodeposition has been indicated as a suitable method since it allows a high control of orientation, shape and morphology of deposited nanostructures by simply adjusting variables such as pH, applied potential or intensity, bath temperature [20, 21] or concentration of metal ions [22]. Given the above mentioned advantages, the electrochemical deposition has been preferred for the fabrication of Cu_2O/ZnO heterojunction cells which exhibited a conversion efficiency ranging 0.007 – 0.2% [3]. However, while Cu_2O/ZnO heterojunction is widely considered for solar cells, a large variation in the short-circuit current density and power conversion efficiency is exhibited due to Cu_2O layer synthesis [18] and poor interface quality and defects [23].

It is known that parameters including the particle size, crystal faces and crystallinity of Cu_2O determine the junction interface and consequently the solar cell performance. Thus, proper conditions must be found for the deposition of Cu_2O film. It has already been demonstrated that the sequence involving deposition of ZnO followed by Cu_2O film results in better current-voltage characteristics due to smaller lattice mismatch and the induced growth of Cu_2O crystals with (111) preferential orientation [24].

In the present work, Cu_2O/ZnO heterojunction was prepared on fluorine-doped tin oxide (FTO) substrate by using a combined approach: the tape-casting technique for the preparation of ZnO film and electrodeposition for the Cu_2O one. The properties of such heterojunction were evaluated with the presence of GO which was employed in order to improve the properties of ZnO film and with the presence of an electrodeposited buffer layer (ZnO) introduced in order to improve the ZnO/Cu_2O interface properties. Detailed investigation on the effects of such approach on the electrochemical growth, structural and optical properties of the heterojunction is presented. Given that the absorption of light in these devices is also controlled by the thickness of the active layer, the photovoltaic characteristics were also studied for tape-cast ZnO film with varying thickness. To the best of our knowledge, there is no report on the properties of Cu_2O/electrodeposited ZnO/tape-cast GO-modified ZnO heterojunction solar cell.

2. Materials and Methods

2.1. Materials. Zinc oxide (ZnO), ethylene glycol ($C_2H_6O_2$), zinc chloride ($ZnCl_2$), potassium chloride (KCl), copper (II) sulphate pentahydrate ($CuSO_4{\cdot}5H_2O$, 85%), lactic

acid ($C_3H_6O_3$, 85%), sodium hydroxide (NaOH) were purchased from Panreac. All chemicals were reagent grade and used as received. Graphene oxide aqueous suspension was purchased from Sigma Aldrich. The samples were prepared on the fluorine-doped tin oxide (FTO) substrates (15 Ω/sq.). Prior to the depositions, the FTO substrates were subsequently degreased in a detergent solution, deionized water, isopropanol and ethanol in an ultrasonic bath for 15 min each. Finally, the substrates were dried under N_2.

2.2. Tape-casting of ZnO and ZnO-rGO films. A ZnO paste containing 1 g of ZnO (particle diameter of about 0.67 μm) dispersed in 250 μl of ethylene glycol and 200 μl of distilled water was spread onto previously cleaned FTO substrates by using the doctor blade technique (tape-casting) and spacers in order to achieve ZnO_{DB} films with 5 μm thickness. After drying in air, the film was annealed in a furnace at 350 ºC for 60 min [7, 13].

A similar approach was followed for the ZnO_{DB}-rGO composite film, by adding 200 μl of GO suspension (0.1 mg/ml) to the ZnO paste by sonication for 20 min. The subsequent annealing treatment allowed the partial removal of oxygen functional groups in GO, thus a ZnO_{DB}-rGO film was obtained.

2.3 Electrodeposition of ZnO buffer layer. A conventional three-electrode set-up was employed to electrodeposit a ZnO layer (ZnO_{ED}) onto the ZnO_{DB} film from a solution consisting in 5 mM $ZnCl_2$ and 0.1 M KCl saturated with O_2. The plating solution was maintained at 75 ºC using a water bath. The pH value of the as-prepared solution was 6. The electrodeposition was performed at a constant potential of -0.8 V [25] for 20 min.

2.4 Electrodeposition of Cu_2O film. The Cu_2O/ZnO_{DB} and Cu_2O/ZnO_{DB}-GO heterojunctions were prepared by electrochemical deposition method. The Cu_2O film was electrodeposited onto the ZnO_{DB} and ZnO_{DB}-rGO film, respectively, from a solution consisting of 0.4 M $CuSO_4$, 3 M $C_3H_6O_3$, and 4 M NaOH. The plating solution was maintained at 35 ºC using a water bath in order to obtain cube-like morphology, given that this exhibits the highest absorbancy. The electrodeposition was performed at a constant potential of -0.6 V [26] for 180 min. Further, the heterojunction was obtained in the presence of the ZnO buffer layer (ZnO_{ED}).

2.5. Characterization. The electrodepositions were performed by using a potentiostat (Autolab) and NOVA software. A Pt foil was employed as counter electrode and an

Ag/AgCl in saturated KCl as a reference one. Structural characteristics were measured by X-ray diffraction (XRD) with a diffractometer (Rigaku Ultima IV) in the Bragg-Bentano configuration using Cu Kα radiation (1.54 Å). The cross-section images were analyzed by using Field Emission Scanning Electron Microscopy (FESEM, Bruker) working at a 2kV. Raman spectroscopy was performed on a LabRam HR UV spectroscope using a He-Ne (632.8 nm) laser with a 1.6 cm^{-1} resolution. The solar cells were sealed with conductive carbon cement (Leit-C). The photoelectrical properties were performed by using potentiostat (Autolab) equipped with AM 1.5G illumination from a calibrated solar simulator with irradiation intensity of 100 mW/cm^2 at 25 ºC.

3. Results y discussion

3.1. Electrodeposition of ZnO buffer layer and the Cu_2O film

Figure 1a depicts de electrodeposition curves for the synthesis of the ZnO buffer layer onto the ZnO_{DB} film. The effect of GO addition to the tape-cast film on the electrodeposition of buffer layer was studied. As one can observe, the current transients show a plateau value indicating a homogeneous growth in both cases. The electrodeposition of ZnO onto a ZnO_{DB}-rGO film results in a lower plateau current, being attributed to the lower conductivity of rGO sheets in the composite.

In order to fabricate the Cu_2O/ZnO heterojunctions, a Cu_2O film was electrodeposited onto the surface of tape-cast ZnO_{DB} film and further compared with the ZnO_{DB}-GO one (figure 1b). The interface between the two films was studied by introducing the ZnO buffer layer (figure 1c). As previously observed, the presence of low-conductivity partially-reduced GO nanosheets in the tape cast ZnO_{DB} film resulted in lower plateau growth current values, indicative of lower thickness Cu_2O film, also due to the fact that the protruding rGO nanosheets serve as nucleation sites due to their decoration with residual oxygen functional groups [16].

On the other hand, the presence of the ZnO buffer layer on top of tape-cast films resulted in an improved nucleation of the Cu_2O nanocrystals (figure 1c) which can be attributed to a lower lattice mismatch.

3.2. Structure analysis

Figure 2 depicts the XRD spectrum evolution of the Cu_2O/ZnO_{DB} heterojunctions fabricated on the FTO substrate. The addition of GO to the tape-cast film and that of ZnO buffer layer at the interface were studied. The obtained patterns indicate besides

the peaks of FTO substrate also the crystalline structure of the heterojunctions. GO presence is not observed in the spectra due to the low amount in the matrix [13].

The hexagonal wurtzite ZnO is identified by the presence of (100), (002), (101), (102), (110), (103) and (201) reflections (in agreement with JCPDS 00-036-1451) with a strong c-axis orientation [22]. The electrodeposition of a ZnO buffer layer results in a random orientation of nanocrystals being indicative of high roughness of the tape cast ZnO film. Moreover, the addition of GO into the tape-cast film results in a lower (002) texture coefficient for ZnO, which can be attributed to electrochemical growth of ZnO nanocrystals onto the protruding GO sheets.

The Cu_2O cubic-structured is indicated by the presence of (111), (310), (222) reflections in agreement with JCPDS 00-005-0667 [27]. The presence of buffer layer appears to affect the orientation of electrodeposited Cu_2O nanocrystals, that is, in the presence of ZnO buffer layer, the (110), (200), (220), (311) peaks of Cu_2O disappear while slightly smaller particle size is obtained.

The overlapping of the Cu_2O (111) and ZnO (101) [22] and the slight angle shift of the Cu_2O peak with the presence of the buffer layer are indicative of strong interface properties.

3.3. Morphology analysis

In order to study the morphology of the heterojunctions, transversal images were collected by FESEM microscopy, as depicted in figure 3. Besides a high homogeneity clearly distinguished in all cases, a continuous interface can be observed between the tape-cast ZnO and electrodeposited Cu_2O film.

The smaller size crystals and compactness observed in inset of figure 3b is indicative for the electrodeposition of ZnO buffer layer at the interface between the two films. The change in the orientation of Cu_2O crystals due to the presence of ZnO buffer layer can also be noted in figure 3b, in agreement with XRD results.

On the other hand, the addition of GO nanosheets is observed to induce a higher porosity to the tape-cast ZnO film (figure 3c and d) which can be due to the partial removal of adsorbed water and oxygen functional groups in GO nanosheets by annealing treatment. The increased porosity of ZnO_{DB} film in figure 3d is attributed not only to the partial reduction of GO by annealing but also due to the electrochemical reduction of the GO sheets during the deposition of ZnO buffer layer.

3.4. Raman analysis

The Raman spectrum evolution of ZnO films with the presence of GO and the ZnO buffer layer are shown in figure 4a. All Raman scattering spectra are dominated by E2 (low) mode at 100 cm^{-1} and E2 (high) mode at 439 cm^{-1}, which are associated with the vibration of the heavy Zn sub-lattice and oxygen atoms, respectively, and thus, indicative of perfect crystal quality [28]. The spectra also show other peaks at about 333 cm^{-1} assigned to E2 (high) – E2 (low) mode, a peak at 382 cm^{-1} which is attributed to A1(TO) mode, one at 541 cm^{-1} which corresponds to 2B1(LO) overtone [29] and another one at 585 cm^{-1} which is attributed to the E1(LO) phonon that appears when the c-axis of the wurtzite ZnO is perpendicular on the sample surface [28, 30].

One of the features of the spectra is that the intensity of the E2 (high) mode decreases with the presence of GO and the buffer layer, due to potential fluctuations of the ZnO disorder. The tape-cast film and the composite tape-cast film show a redshift in the E2 (high) mode suggesting a compressive stress [31]. However, the electrodeposition of a buffer layer resulted in lower red shift of the mode with respect to the theoretical values.

Another feature is that the Raman band at 500–650 cm^{-1} gets stronger. Considering that the E1(LO) mode is most affected by the presence of impurities and/or defects [32], the addition of GO and buffer layer have opposite effects, that is the former results in a red shift of the peak with respect to theoretical value, suggesting an oxygen deficiency in ZnO, and an opposite effect by the latter.

On the other hand, the typical Raman features of GO are revealed in the tape-cast composite films, as depicted in figure 4b. In comparison to GO, the spectra of tape-cast composite film show a red shift of the D band, a blue shift of the G band – both being more pronounced upon electrodeposition of the buffer layer, as well as a decrease in the intensity ratio between the D and G bands, thus suggesting a partial removal of oxygen functional groups and an increase in the average size of sp^2 hybridized carbon domains [33].

3.5. Photoelectric properties

The characteristic current-voltage (I-V) curves of the Cu_2O/ZnO heterojunctions are depicted in figure 5. The corresponding short-circuit current density (J_{SC}) and the open circuit voltage (V_{OC}) are listed in table 1. It was observed the Cu_2O/ZnO_{DB} heterojunction exhibits lower J_{SC} in presence of a buffer layer, while the addition of GO

to the tape-cast ZnO film results in a 1.5 fold J_{SC} and a small decrease in V_{OC}. The improvement observed in the presence of GO can be attributed to an impeded electron-hole recombination and a faster electron transport due to the presence of partially reduced GO nanosheets in the ZnO active layer while the lower characteristics observed in the presence of buffer layer could be explained by the losses through recombination and by an increased resistivity of the ZnO film [3],[34]. In the case of a composite ZnO-GO film modified with a buffer layer, a decrement in V_{OC} value and a 5-fold J_{SC} of the initial value were observed, in agreement with the previous findings. The obtained results are in accordance to the literature, graphene (or reduced GO) addition to similar heterojunctions being accounted for the charge transfer enhancement as it can serve as a channel for the photogenerated carriers [35] [36]. A clear enhancement can be observed by adding GO to the ZnO film, as it can be seen from the comparison with other works, as presented in table 2.

Considering that the light absorption increases with active layer thickness and that the charge recombination increases with the resistivity [37], the effect of GO addition was studied for an increased thickness of the tape-cast ZnO film (2-folds), as well. An experimental design was created (considering the following parameters at two levels: A - thickness of ZnO_{DB}, B - addition of GO, C - addition of a buffer layer) in order to optimise the process and indicate useful trends. The current and voltage outputs considered as response variables were analysed with Yates algorithm (STATGRAPHICS Plus. v5.0). It was observed that both individual parameters and combined ones are significant. Thus, while the thickness of tape-cast ZnO and the addition of a buffer layer seem detrimental for the voltage response, the addition of GO appears to improve the voltage, in agreement with the obtained results. Moreover, variance analysis (ANOVA) was performed and the results for response variables are as presented in tables 3 and 4. In this case, the significance of the thickness of tape-cast ZnO for the output voltage appeared to be 94%, while the addition of GO and the buffer layer were significant as 91.4% and 95%, respectively. The significance of combined parameters resulted to be greater for the ZnO thickness together with GO addition or presence of both GO and buffer layer. On the other hand, the highest significance for the output current was the GO addition (86%). These results could be explained by the fact that increasing the tape-cast ZnO thickness, the probability for defects or discontinuities increases while the addition of GO could help in increasing the

conductivity properties thanks to the partial reduction by thermal treatment and electroreduction. An improved dispersion of GO sheets could have synergetic effects with the ZnO buffer layer towards improved growth of the Cu_2O film and increased junction area. On the other hand, a proper balance between the active layer thickness and the GO content with a higher reduction degree could be considered as a proper approach in order to improve the solar cell performance.

The proposed approaches for the fabrication of the Cu_2O/ZnO heterojunction could be further applied to other conductive substrates (tin-doped indium oxide, metalized substrates) [38] for photovoltaic application by taking into account also the roughness of the substrate. In order to better control the nanostructuring of ZnO active layer and the junction area, one should adjust the particle size of ZnO material or employ the electrodeposition technique, where ZnO would form as nanocolumns, nanorods or nanotubes.

4. Conclusions

The fabrication of Cu_2O/ZnO heterojunction, using tape-casting (or doctor Blade, DB) of ZnO film is reported. The influence of GO addition to the tape-cast film and introduction of a ZnO buffer layer by electrochemical deposition at the interface were studied. The morphology measurements indicated larger porosity for the tape-cast film with addition of GO and a varying structure and orientation of Cu_2O crystals with the presence of buffer layer, respectively. The photoelectrical measurements indicated the performance of the solar cell improves with the addition of GO to the ZnO active layer. While more work need to be performed, the sensitization of ZnO film with GO seems a promising approach for improving Cu_2O/ZnO heterojunction solar cells performance.

Acknowledgements

Financial support from Escuela Politécnica Nacional (project number PIMI 15-09) and Secretaría de Educación Superior, Ciencia, Tecnología e Innovación (SENESCYT) and Romanian National Authority for Scientific Research and Innovation, CNCS – UEFISCDI (project number PN-III-P1-1.1-TE-2016-1544) is gratefully acknowledged.

References:

1. Yu L, Xiong L, Yu Y (2015) Cu2O Homojunction Solar Cells: F-Doped N-type Thin Film and Highly Improved Efficiency. J Phys Chem C 119:22803–22811. doi: 10.1021/acs.jpcc.5b06736

2. Jiang X, Lin Q, Zhang M, et al (2015) Microstructure, optical properties, and catalytic performance of Cu2O-modified ZnO nanorods prepared by electrodeposition. 2–7. doi: 10.1186/s11671-015-0755-0

3. Ke NH, Trinh LTT, Phung PK, et al (2016) Changing the thickness of two layers: i-ZnO nanorods, p-Cu2O and its influence on the carriers transport mechanism of the p-Cu2O/i-ZnO nanorods/n-IGZO heterojunction. Springerplus 5:710. doi: 10.1186/s40064-016-2468-y

4. Gunnaes AE, Gorantla S, Lovvik OM, et al (2016) Epitaxial Strain-Induced Growth of CuO at Cu2O/ZnO Interfaces. J Phys Chem C 120:23552–23558. doi: 10.1021/acs.jpcc.6b07197

5. Jabbari M, Bulatova R, Tok AIY, et al (2016) Ceramic tape casting: A review of current methods and trends with emphasis on rheological behaviour and flow analysis. Mater Sci Eng B Solid-State Mater Adv Technol 212:39–61. doi: 10.1016/j.mseb.2016.07.011

6. Dong Q, Zhu T, Xie Z, et al (2017) Optimization of the tape casting slurries for high-quality zirconia substrates. Ceram Int 43:16943–16949. doi: 10.1016/j.ceramint.2017.09.099

7. Saito M, Fujihara S (2009) Fabrication and photovoltaic properties of dye-sensitized ZnO thick films by a facile doctor-blade printing method using nanocrystalline pastes. J Ceram Soc Japan 117:823–827. doi: 10.2109/jcersj2.117.823

8. Williams JC (1976) Doctor-Blade Process. In: Wang F (ed) Ceram. Fabr. Process. Treatise Mater. Sci. Technol. Academic Press, New York, pp 173–198

9. Albano MP, Garrido LB (2005) Influence of the slip composition on the properties of tape-cast alumina substrates. Ceram Int 31:57–66. doi: 10.1016/j.ceramint.2004.03.035

10. Sima C, Grigoriu C, Toma O, Antohe S (2015) Study of dye sensitized solar cells based on ZnO photoelectrodes deposited by laser ablation and doctor blade

methods. Thin Solid Films 597:206–211. doi: 10.1016/j.tsf.2015.11.051

11. Siddick SZ, Lai CW, Juan JC, Hamid SB (2017) Reduced Graphene Oxide - Titania Nanocomposite Film for Improving Dye-Sensitized Solar Cell (DSSCs) Performance. Curr Nanosci 13:494–500. doi: 10.2174/1573413713666170519123159

12. Retnaningsih L, Muliani L (2016) The result of synthesis analysis of the powder TiO2/ZnO as a layer of electrodes for dye sensitized solar cell applications. AIP Conf Proc. doi: 10.1063/1.4945523

13. Chang W-C, Tseng T-C, Yu W-C, et al (2016) Graphene/ZnO nanoparticle composite photoelectrodes for dye-sensitized solar cells with enhanced photovoltaic performance. J Nanosci Nanotechnol 16:9160–9165. doi: 10.1166/jnn.2016.12900

14. Abbasi HY, Habib A, Tanveer M (2017) Synthesis and characterization of nanostructures of ZnO and ZnO/Graphene composites for the application in hybrid solar cells. J Alloys Compd 690:21–26. doi: 10.1016/j.jallcom.2016.08.161

15. Pruna A, Wu Z, Zapien JA, et al (2018) Enhanced photocatalytic performance of ZnO nanostructures by electrochemical hybridization with graphene oxide. Appl Surf Sci. doi: 10.1016/j.apsusc.2018.02.117

16. Pruna A, Shao Q, Kamruzzaman M, et al (2016) Optimized properties of ZnO nanorod arrays grown on graphene oxide seed layer by combined chemical and electrochemical approach. Ceram Int 42:17192–17201. doi: 10.1016/j.ceramint.2016.08.011

17. Wang P, Wu H, Tang Y, et al (2015) Electrodeposited Cu2O as Photoelectrodes with Controllable Conductivity Type for Solar Energy Conversion. J Phys Chem C 119:26275–26282. doi: 10.1021/acs.jpcc.5b07276

18. Perng DC, Hong MH, Chen KH, Chen KH (2017) Enhancement of short-circuit current density in Cu2O/ZnO heterojunction solar cells. J Alloys Compd 695:549–554. doi: 10.1016/j.jallcom.2016.11.119

19. Switzer JA, Kothari HM, Bohannan EW (2002) Thermodynamic to kinetic transition in epitaxial electrodeposition. J Phys Chem B 106:4027–4031. doi:

10.1021/jp014638o

20. Liu R, Bohannan EW, Switzer J a, et al (2003) Shape Control in Epitaxial Electrodeposition: Cu_2O on InP(001). Chem Mat 83:1944–1946. doi: 10.1063/1.1606503

21. Siegfried MJ, Choi KS (2005) Directing the architecture of cuprous oxide crystals during electrochemical growth. Angew Chemie - Int Ed 44:3218–3223. doi: 10.1002/anie.200463018

22. Lahmar H, Setifi F, Azizi A, et al (2017) On the electrochemical synthesis and characterization of p-Cu2O/n-ZnO heterojunction. J Alloys Compd 718:36–45. doi: 10.1016/j.jallcom.2017.05.054

23. Jeong SS, Mittiga A, Salza E, et al (2008) Electrodeposited ZnO/Cu2O heterojunction solar cells. Electrochim Acta 53:2226–2231. doi: 10.1016/j.electacta.2007.09.030

24. Akimoto K, Ishizuka S, Yanagita M, et al (2006) Thin film deposition of Cu2O and application for solar cells. Sol Energy 80:715–722. doi: 10.1016/j.solener.2005.10.012

25. Cembrero J, Perales M, Mollar M, Marí B (2003) Obtención de columnas de ZnO. Variables a controlar (I). Boletín la Soc Española Cerámica y Vidr 42:379–397.

26. Cembrero-Coca P, Cembrero J, Busquets-Mataix D, et al (2017) Factorial electrochemical design for tailoring of morphological and optical properties of Cu<inf>2</inf>O. Mater Sci Technol (United Kingdom). doi: 10.1080/02670836.2017.1349595

27. Septina W, Ikeda S, Khan MA, et al (2011) Potentiostatic electrodeposition of cuprous oxide thin films for photovoltaic applications. Electrochim Acta 56:4882–4888. doi: 10.1016/j.electacta.2011.02.075

28. Zhang R, Yin P-G, Wang N, Guo L (2009) Photoluminescence and Raman scattering of ZnO nanorods. Solid State Sci 11:865–869. doi: 10.1016/j.solidstatesciences.2008.10.016

29. Cuscó R, Alarcón-Lladó E, Ibáñez J, et al (2007) Temperature dependence of Raman scattering in ZnO. Phys Rev B 75:165202. doi:

10.1103/PhysRevB.75.165202

30. Alim KA, Fonoberov VA, Balandin AA (2005) Origin of the optical phonon frequency shifts in ZnO quantum dots. Appl Phys Lett 86:053103. doi: 10.1063/1.1861509

31. Huang Y, Liu M, Li Z, et al (2003) Raman spectroscopy study of ZnO-based ceramic films fabricated by novel sol–gel process. Mater Sci Eng B 97:111–116. doi: 10.1016/S0921-5107(02)00396-3

32. Šćepanović M, Grujić-Brojčin M, Vojisavljević K, et al (2010) Raman study of structural disorder in ZnO nanopowders. J Raman Spectrosc 41:914–921. doi: 10.1002/jrs.2546

33. Pruna A, Shao Q, Kamruzzaman M, et al (2016) Enhanced electrochemical performance of ZnO nanorod core/polypyrrole shell arrays by graphene oxide. Electrochim Acta 187:517–524. doi: 10.1016/j.electacta.2015.11.087

34. Kang D, Lee D, Choi K-S (2016) Electrochemical Synthesis of Highly Oriented, Transparent, and Pinhole-Free ZnO and Al-Doped ZnO Films and Their Use in Heterojunction Solar Cells. Langmuir 32:10459–10466. doi: 10.1021/acs.langmuir.6b01902

35. Bai Z, Liu J, Liu F, Zhang Y (2017) Enhanced photoresponse performance of self-powered UV–visible photodetectors based on ZnO/Cu2O/electrolyte heterojunctions via graphene incorporation. J Alloys Compd 726:803–809. doi: 10.1016/j.jallcom.2017.08.035

36. Wang Y, Wang F, He J (2013) Controlled fabrication and photocatalytic properties of a three-dimensional ZnO nanowire/reduced graphene oxide/CdS heterostructure on carbon cloth. Nanoscale 5:11291. doi: 10.1039/c3nr03969b

37. Lenes M, Koster LJA, Mihailetchi VD, Blom PWM (2006) Thickness dependence of the efficiency of polymer:fullerene bulk heterojunction solar cells. Appl Phys Lett 88:86–89. doi: 10.1063/1.2211189

38. Cui J, Gibson UJ (2010) A Simple Two-Step Electrodeposition of Cu_2O/ZnO Nanopillar Solar Cells. J Phys Chem C 114:6408–6412. doi: 10.1021/jp1004314

39. Panigrahi S, Nunes D, Calmeiro T, et al (2017) Oxide-Based Solar Cell: Impact of Layer Thicknesses on the Device Performance. ACS Comb Sci 19:113–120.

doi: 10.1021/acscombsci.6b00154

40. Makhlouf H, Weber M, Messaoudi O, et al (2017) Study of Cu2O\ZnO nanowires heterojunction designed by combining electrodeposition and atomic layer deposition. Appl Surf Sci 426:301–306. doi: 10.1016/j.apsusc.2017.07.130

Table 1. The parameters of different heterojunction solar cells.

Heterojunction	V_{OC} (mV)	J_{SC} (μA/cm^2)
Cu_2O/ZnO_{DB}	100.7	39.3
$Cu_2O/ZnO_{ED}/ZnO_{DB}$	10.8	0.08
Cu_2O/ZnO_{DB}-GO	82.6	103.4
$Cu_2O/ZnO_{ED}/ZnO_{DB}$-GO	53.2	242.5

Table 2. I-V characteristics of Cu_2O/ZnO heterojunction solar cells.

System	**Method**	**V_{oc} (mV)**	**I_{sc} (mA/cm^2)**	**Ref.**
Cu_2O/ZnO/ITO	Spay pyrolysis	60	0.3	[39]
Cu_2O/i-ZnO/n-IGZO	Electrochemical deposition	140 410	0.47 0.21	[3]
Cu_2O/ZnO NWs/ZnO_{ALD}	Atomic layer deposition for ZnO and electrochemical deposition to ZnO NWs and Cu_2O	0.051-0.058	0.009-0.025	[40]
Cu_2O/ZnO-GO/FTO	Tape-casting of ZnO-GO and electrodeposition of Cu_2O layer	53	0.242	This work

Table 3. Analysis of Variance for output variable - voltage

Source	Sum of Squares	Df	Mean Square	F-Ratio	P-Value
A: Factor_A	6728,0	1	6728,0	111,21	**0,0602**
B: Factor_B	3280,5	1	3280,5	54,22	0,0859
C: Factor_C	10082,0	1	10082,0	166,64	**0,0492**
AB	3612,5	1	3612,5	59,71	0,0819
AC	450,0	1	450,0	7,44	0,2237
BC	8064,5	1	8064,5	133,30	0,0550
Total, error			60,5	1	60,5
Total (corr.)	32278,0	7			

Table 4. Analysis of Variance for output variable - current

Source	Sum of Squares	Df	Mean Square	F-Ratio	P-Value
A: Factor_A	9045,13	1	9045,13	5,11	0,2652
B: Factor_B	30876,1	1	30876,1	17,44	0,1496
C: Factor_C	2145,13	1	2145,13	1,21	0,4695
AB	21528,1	1	21528,1	12,16	0,1778
AC	10,125	1	10,125	0,01	0,9519
BC	5356,13	1	5356,13	3,03	0,3322
Total, error			1770,13	1	1770,13
	Total (corr.)		70730,9	7	

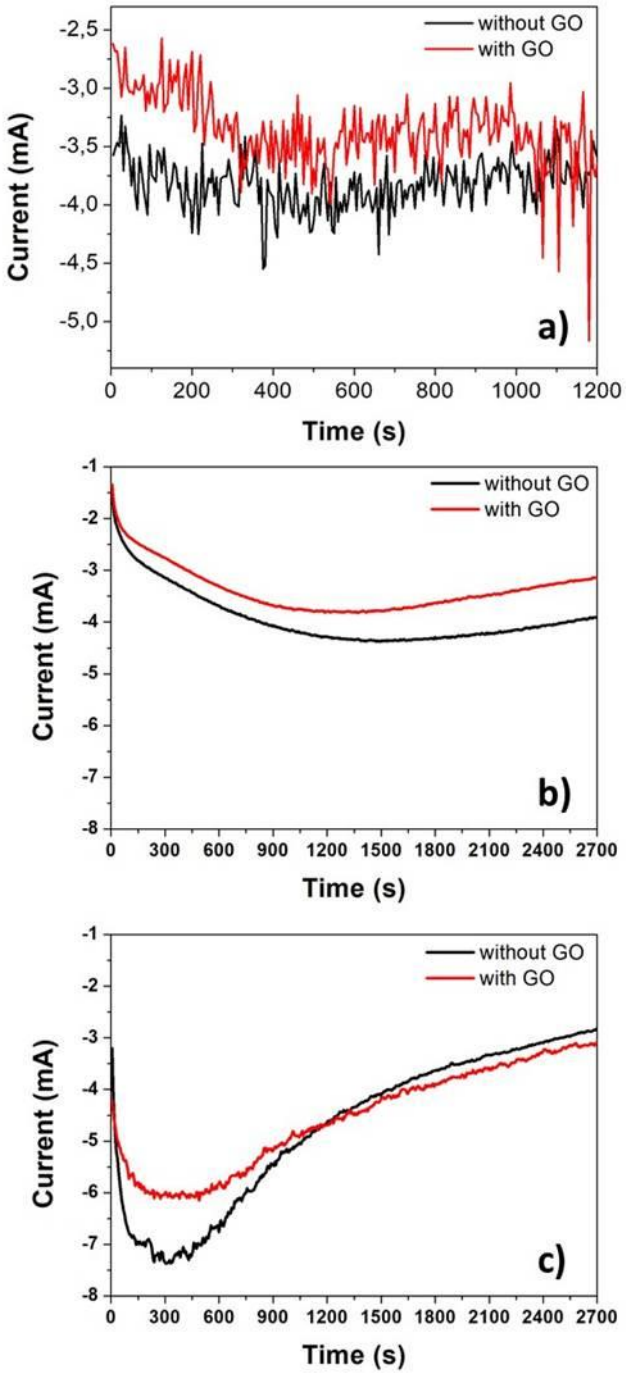

Fig. 1. Current transients for the electrodeposition of ZnO buffer layer onto tape-cast ZnO_{DB} film (a); Cu_2O onto tape-cast ZnO_{DB} film in absence (b) and presence of ZnO buffer layer (c). Effect of GO addition to the tape-cast ZnO_{DB} film highlighted.

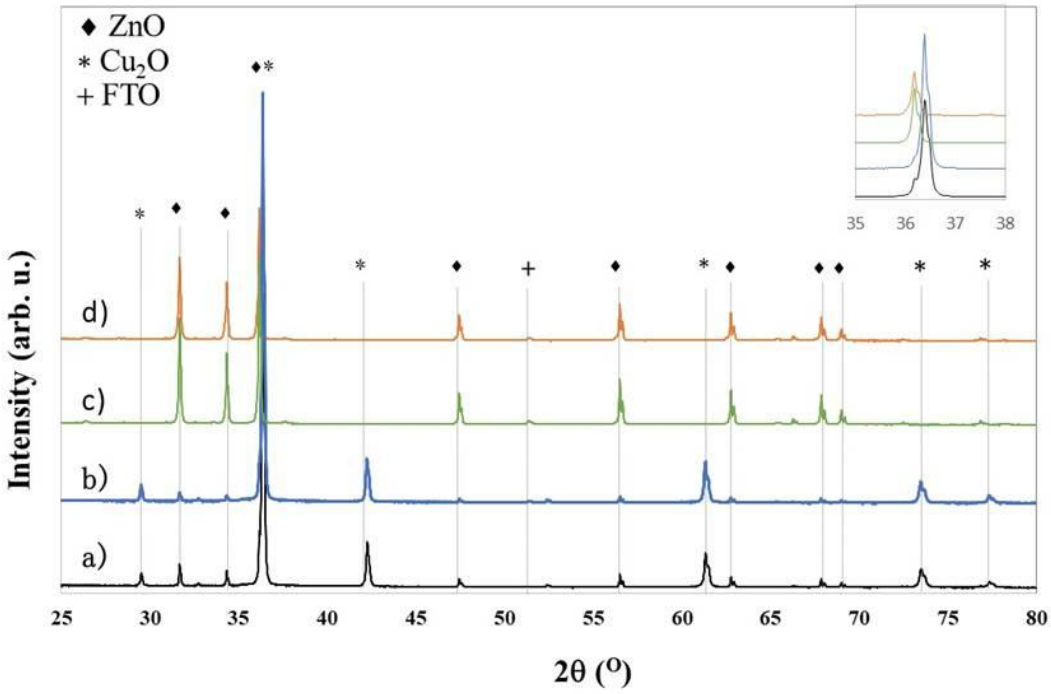

Fig. 2. X-ray diffraction pattern of Cu_2O/ZnO_{DB} in absence of buffer layer, without GO (a), with GO (b) and in presence of buffer layer without GO (c) and with GO (d).

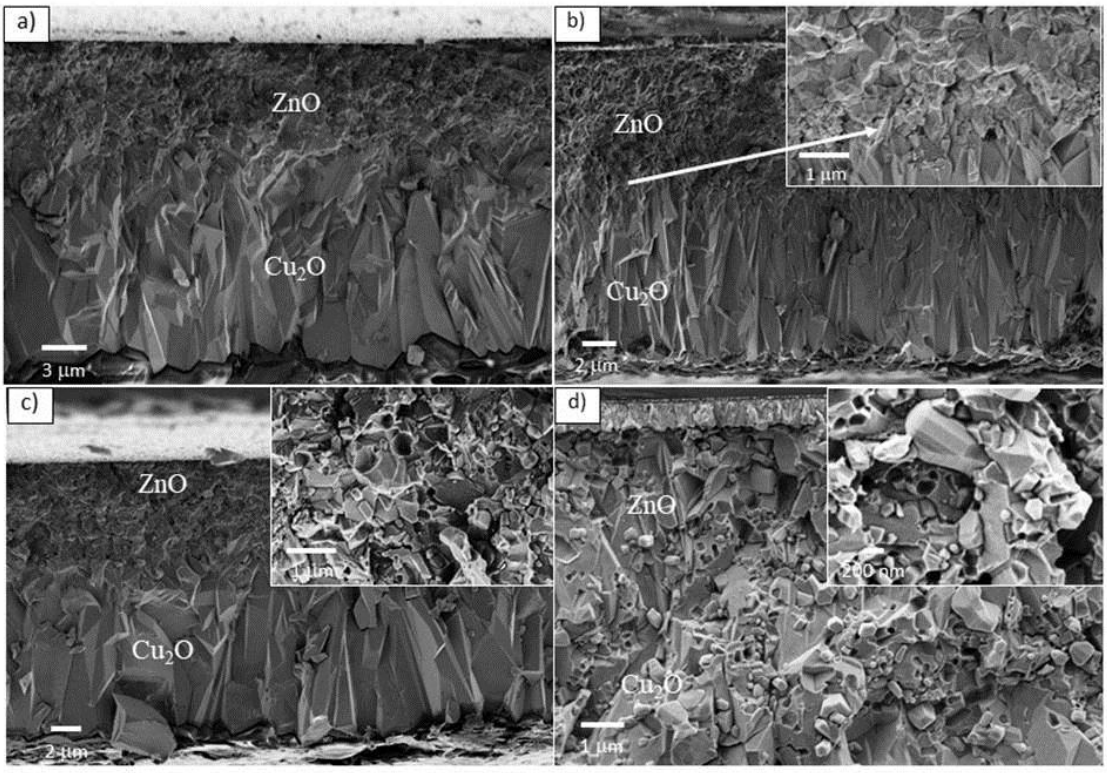

Fig. 3. FESEM section images of the Cu_2O/ZnO_{DB} heterojunctions in absence (a) and presence of buffer layer (b) and Cu_2O/ZnO_{DB}-GO in absence (c) and presence of buffer layer (d).

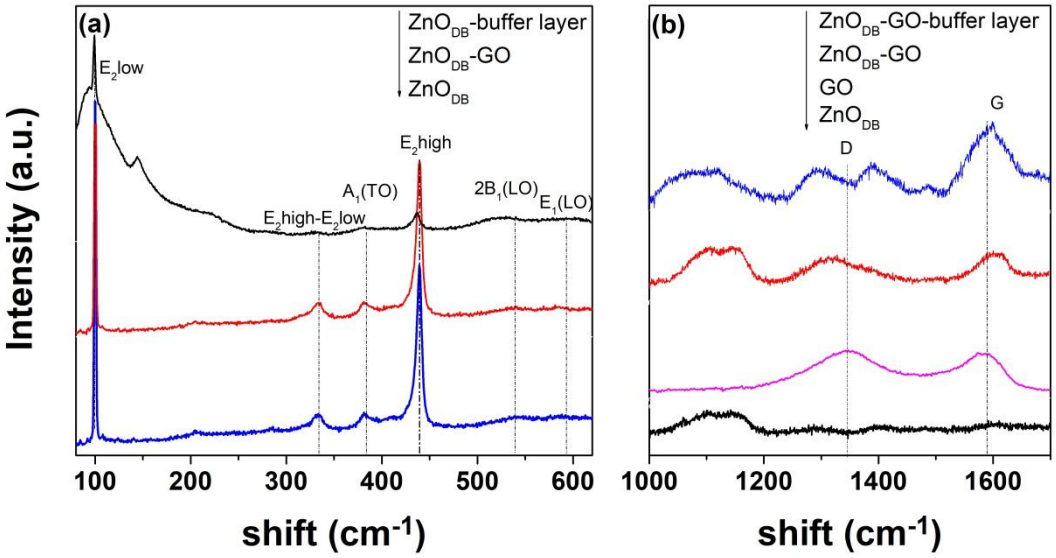

Fig. 4. Raman spectra of GO in the tape-cast films.

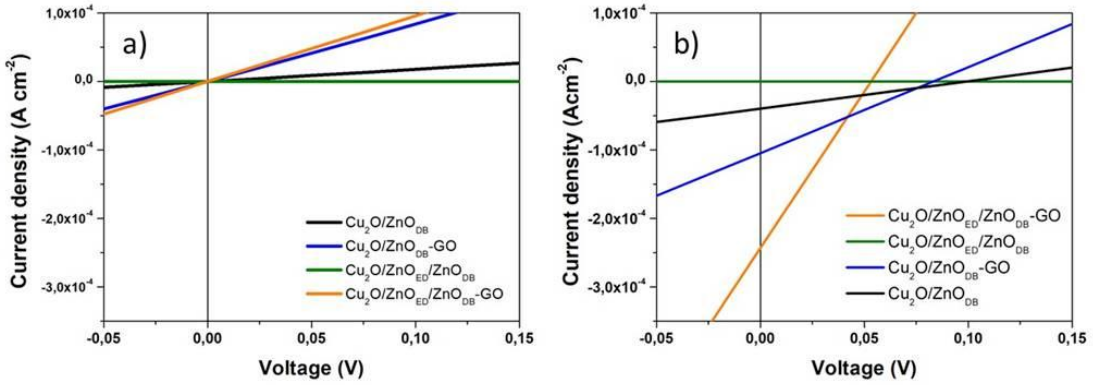

Fig. 5. Typical I-V curves of the Cu_2O/ ZnO heterojunctions without (a) and with illumination (b).